# Soil Moisture Mapping Based on Temperature-Soil Moisture Dryness Index - a case study for the tailing dam in Brumadinho, Brazil

Yu Lan, Jens-André Paffenholz

Institute of Geo-Engineering, Clausthal University of Technology, Germany, (yu.lan@tu-clausthal.de; jens-andre.paffenholz@tu-clausthal.de)

**Key words**: *Soil moisture*; *Tailing dam*; *Brumadinho*; *TMDI*; *TVDI; ET; Landsat8*

**ABSTRACT**

The tailing dam in Brumadinho of Brazil collapsed on 25th January 2019, it caused serious casualties and environmental pollution. The monitoring of the tailing dam stability has become an urgent problem. For monitoring, soil moisture is an important parameter, if the soil moisture is too high, it will cause soil liquefaction and then the stability of the tailing dam will decrease. In this study, Landsat 8 data is innovatively used to calculate the Temperature-Soil Moisture Dryness Index (TMDI) for the estimation of soil moisture of the collapsed tailing dam in Brumadinho. The data on 14th January 2019 and 30th January 2019 are used in order to better understand the soil moisture before and after the collapse of tailing dam. TMDI is calculated based on triangle space of Land Surface Temperature (LST) and Normalized Difference Latent Heat Index (NDLI). This new index TMDI is used for the assessment of the soil moisture and evapotranspiration (ET). The performance of TMDI and Temperature Vegetation Dryness Index (TVDI) are evaluated by the reference evapotranspiration (ET), which is calculated based on the Surface Energy Balance Algorithm for Land (SEBAL). Results of the correlation between TMDI, TVDI and SEBAL-derived ET indicate that TMDI is a better index for estimating soil moisture. The built-up region shows high negative correlation with SEBAL-derived ET. According to the spatial distribution of TMDI and TVDI, in the tailing dam, some parts of the dam body shows high soil moisture which may have the potential risk of soil liquefaction.

## I. INTRODUCTION

Tailing dam in Brumadinho was damaged on 25th January 2019, it released mudflow into the local place and even the river, this accident caused great losses. Soil liquefaction may be one of the potential reasons for the loss of stability of the tailing dam. Estimation of soil moisture of an area is very important, not only in agriculture but also in monitoring geological hazard. Remote sensing technology is a good method to monitor the geological hazard, for example, high soil moisture monitoring and deformation detection etc.

For the tailing dam in Brumadinho, based on Landsat data, (Rotta *et al.*, 2020) used the Temperature Vegetation Dryness Index (TVDI) as the indicator to get the soil moisture of the tailing dam. They observed high soil moisture over the Top-of-bench sector of the dam. Besides, they also used Sentinel-1 data to get a time-series of the tailing dam's deformation. They found cumulated displacements between 3rd January 2018 and 22nd January 2019 (Gama *et al.*, 2020) used Differential Interferometric Synthetic Aperture Radar (DInSAR) to monitor the surface deformation of the tailing dam. They used Small BAseline Subset (SBAS) and Persistent Scatterer Interferometry (PSI) in their analysis. The Digital SurfaceModel (DSM) was applied to remove the topographic phase component. They found that the maximum displacement was detected along the downstream slope face, they were 39 mm with SBAS and 48 mm with PSI, respectively.

Surface water can absorb the radiation from sun and can convert this kind of energy into latent heat in the form of evapotranspiration (ET). Therefore, surface water has the capability to moderate Land Surface Temperature (LST) (Qiu *et al.*, 2013). If the amount of the surface water is limited, it will induce the constraining of the latent heat transfer, then the LST will easily increase. Based on the correlation between LST and water content, researchers applied the triangle space method to extract the land surface information based on LST and some other indices (Le and Liou, 2021). The most common index researchers used is TVDI, which is based on the triangle space of Normalized Difference Vegetation Index (NDVI) and LST. TVDI is widely used in the agriculture field. TVDI is inversely proportional to soil moisture, which means, the higher the index is, the lower the soil moisture will be. Recently, (Le and Liou, 2021) found the Temperature-Soil Moisture Dryness Index (TMDI), which proved to be a better index in comparison with TVDI. The TMDI is calculated based on the triangle space of Normalized Difference Latent Heat Index (NDLI) and LST. They applied this index to estimate the soil moisture in an alluvial plain located along the south-west coast of Taiwan. In their study, the ET derived from the Surface Energy Balance Algorithm for Land (SEBAL) was used as the reference to evaluate the performance of TMDI and TVDI. They found that TMDI shows sensitivity to the surface soil fluctuation. Besides, they also found that TMDI could perform better than TVDI in

the response to the rapid change of soil moisture. (Le and Liou, 2022) also used TMDI to estimate the soil moisture. The performance of the TMDI was evaluated by the SEBAL-derived ET and verified by the near-surface temperature and in-situ humidity. They found TMDI had negative correlation with the SEBAL-derived ET and positive correlation with the in-situ near-surface air temperature. They also compared TMDI with other indices and they found that TMDI has advantage over other indices especially in the non-vegetation area. They concluded that TMDI was a reliable index for the estimation of soil moisture.

The main content of this paper can be summarized as follows: Section II Study area and data; Section III includes the equations for the TMDI and ET calculation; Section IV includes the results of land use and land cover (LULC) classification, index and LST calculation, the correlation analysis and also the spatial distribution of the soil moisture in the tailing dam; Section V shows the conclusion of the study.

## II. Study Area and Data

### A. *Study area*

The study area is the tailing dam at the Córrego do Feijão iron ore mine shown in Figure 1. It is located in Minas Gerais state of Brazil (20°07'11"S 44°07'17"W).

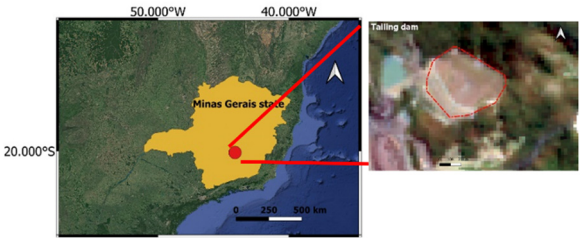


Figure 1. Location of the study area: a) Minas Gerais state (Geofabrik, 2018; Google, n.d.); b) Tailing dam circled in red polygon in Brumadinho generated from Landsat 8 data.

In order to increase the robustness of the calculation of TMDI and TVDI, a larger region, compared to the red polygon in Figure 1b, is clipped for the calculations. The larger region (Figure 2a) includes the whole region of Brumadinho and surrounding areas like Bonfim, Moeda, Rio Manso etc. The tailing dam area is divided into 4 sections (Figure 2b): tailings, dam and the region around the tailings and the region around the dam.

In the tailing dam area shown in Figure 2b, (i) dam is mixed with bare soil and vegetation (grass), (ii) tailings is bare soil with sparse grass, (iii) region around dam is mixed with bare soil and vegetation, (iv) region around tailings is fully covered with vegetation.

The area of each section is shown in the Table 1.

Table 1. Dimension of the Tailing dam

| | i | ii | iii | iv |
|---|---|---|---|---|
| Area ($m^2$) | 91,807 | 251,794 | 182,406 | 285,541 |

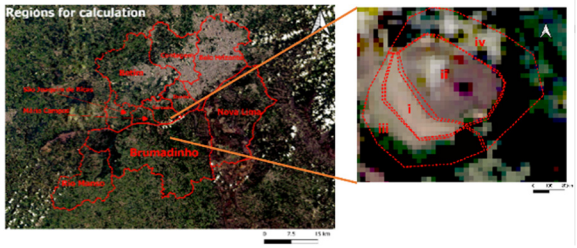


Figure 2. Study area: a) The calculation region of the area; b) Different sections of the tailing dam: (i) dam (ii) tailings (iii) region around dam (iv) region around tailings Both images generated from Landsat 8 data.

### B. *Data*

Landsat 8 data includes the Operational Land Imager (OLI) and the Thermal Infrared Sensor (TIRS) from the United States Geological Survey (USGS). In this paper, Landsat-8 Collection 2 Level-2 Science Products are used (USGS 2022). The data were captured on 14th January 2019 and 30th January 2019 and they are used to estimate the soil moisture of the tailing dam in Brumadinho. The first data was captured before collapse of the tailing dam. Which can get the soil moisture 11 days before collapse. The second image was captured 5 days after the collapse of the tailing dam. In this case, the soil in the tailing dam would be exposed, the soil moisture could also be a reference to check if the soil moisture in the tailings was high or not. Information about the data is shown in the Table 2.

Table 2. Data of Landsat 8

| Platform | Image date | Sensors | Resolution |
|---|---|---|---|
| Landsat 8 | 2019/01/14 | OLI/TIRS | 30 m (OLI)/100 m (TIRS) |
| Landsat 8 | 2019/01/30 | OLI/TIRS | 30 m (OLI)/100 m (TIRS) |

In this study, the data from OLI was used to calculate NDVI and NDLI respectively. The data from TIRS is used to calculate LST.

## III. Methodology

### A. *LULC classification*

The whole region shown in Figure 2a is located between the mine region and Belo Horizonte, which is the capital of Minas Gerais. This region is composed of vegetation and mine area and parts of built-up area and surface water.

LULC classification for this region was used to classify the whole region into several classes: including vegetation, surface water, bare soil, built-up area and cloud (including the cloud shadow). The open-source software Orfeo toolbox (OTB) 7.4.0 is used for the classification. Based on supervised learning, the Support Vector Machines (SVM) classification algorithm was used for the LULC classification.

B. *Index and LST calculation*

TVDI is widely used in the soil moisture estimation. This index is calculated based on NDVI and LST triangle space and it is inversely proportional to the soil moisture. According to the theory from (Le and Liou, 2021), they found another index which could be more sensitive to soil moisture estimation.

TMDI is calculated based on the triangle space of NDLI and LST. The NDLI is proposed for remote sensing of land surface heat flux (Liou *et al*., 2019), it was proved to be a reliable index to determine the water content's characteristics. Therefore, NDLI in this study is used as the indicator for surface water. This index is calculated based on the Equation 1.

$$NDLI = \frac{(\rho_{Green} - \rho_{Red})}{(\rho_{Green} + \rho_{Red} + \rho_{SWIRI})} \quad (1)$$

where $\rho_{Green}$= reflectance of the band 3 (green band)
$\rho_{Red}$ = reflectance of the band 4 (red band)
$\rho_{SWIRI}$= reflectance of the band 6 (short-wave infrared band)

Band 10 in TIRS of Landsat 8 is used to calculate LST. According to the instruction of Landsat 8 Collection-2 Level-2 Science Products (USGS 2022). LST can be calculated by the scaling factor shown in the Equation 2.

$$LST = \mathrm{DN}_{\mathrm{B10}} \cdot 0.00341802 + 149 \quad (2)$$

where $\mathrm{DN}_{B10}$ = digital number of the band 10

C. *NDLI-LST triangle space*

According to the theory from (Le and Liou, 2021) and (Le and Liou, 2022), in certain NDLI interval, the given water can absorb the radiation and then change it into latent heat in the form of ET, in this condition, LST can be decreased because of the cooling effect from ET. This can also directly be connected to soil moisture.

Based on this, a linear regression of LST and NDLI can be applied, the triangle space method is used like NDVI-LST triangle space for calculation of TVDI (Zare *et al*., 2019). In the triangle space of NDLI-LST, the upper limit in the triangle is the dry edge, the lower limit of the triangle is the wet edge. The upper limit and lower limit correspond to the maximum and minimum ET rate (Le and Liou, 2022). With the dry edge and the wet edge, TMDI can be calculated. The equation of TMDI is shown in the Equation 3.

$$TMDI = \frac{(LST - LST_{min})}{(LST_{max} - LST_{min})} \quad (3)$$

where $LST$ = land surface temperature (K)
$LST_{max}$ = maximum LST (K) according to the NDLI along the dry edge
$LST_{min}$ = minimum LST (K) according to the NDLI along the wet edge

The equation of the $LST_{min}$ and $LST_{max}$ are shown below (Eqs. 4 and 5).

$$LST_{max} = a_1 + b_1 \cdot NDLI \quad (4)$$

$$LST_{min} = a_2 + b_2 \cdot NDLI \quad (5)$$

where $a_1$, $b_1$, $a_2$ and $b_2$ = fitting equation coefficients

There is no classification standard for TMDI, but based on the empirical classification from TVDI (Sha *et al*., 2014), the classification for TMDI is set to the values given in Table 3.

Table 3. Classification standard of TMDI

| Extremely humid | Humid | Normal | Slightly dry | Dry |
|---|---|---|---|---|
| 0 to 0.2 | 0.2 to 0.4 | 0.4 to 0.6 | 0.6 to 0.8 | 0.8 to 1 |

D. *ET-based evaluation*

According to (Le and Liou, 2021), in the NDLI-LST triangle space, LST decreases as the ET increases in a certain amount of water. The variation of LST is because of the cooling effect by ET. Based on this, ET is used as the reference data to evaluate the performance of the TMDI and the TVDI. ET is derived from SEBAL and ET data is available at geeSEBAL (Laipelt *et al*., 2021). The equation is shown in Equation 6.

$$\lambda ET = R_n - H - G \quad (6)$$

where ET = evapotranspiration (mm $H^{-1}$)
$\lambda$ = latent heat of vaporization (MJ/kg)
$R_n$ = net radiation ($Wm^{-2}$)
H = sensible heat flux ($Wm^{-2}$)
G = soil heat flux ($Wm^{-2}$)

## IV. Results and Dicussion

A. *LULC classification*

Based on the supervised learning in the OTB 7.4.0, the results of the LULC classification on 14th January 2019 and 30th January 2019 are shown in Figure 3.

From the results shown above, it is obvious that the vegetation represents a large proportion of the whole study area. Vegetation comprises 67%. The built-up area is 24%. Bare soil occupies about 7% of the whole area and the surface water accounts for 1%.

On 30th January 2019, vegetation accounts for 69% of the whole area, bare soil makes up 7%. Built-up occupies 22% while the surface water is 1%.

The accuracy of the LULC classification can be assessed with the Semi-Automatic Classification Plugin (SCP) in QGIS 3.24.1. For the first LULC classification on 14th January 2019, in the LULC

classification result randomly selected fifty samples and tested as well as verified, the overall accuracy is 95.67% and kappa hat classification is 0.91. For the data of 30th January 2019, the overall accuracy is 94.11% and kappa hat classification is 0.88.

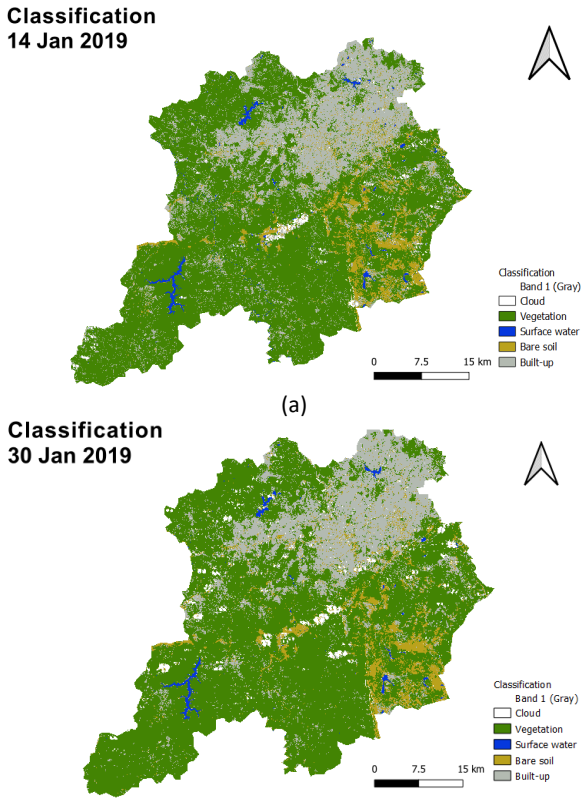


Figure 3. Results of LULC classification: a) result on 14th January 2019; b): result on 30th January 2019.

B. *Index and LST calculation*

The results of the NDLI and LST are used to generate the NDLI-LST triangle space. The result of the NDLI on 14th January 2019 is shown in Figure 4. NDLI ranges from -1 to 1. In the image of NDLI, in order to eliminate the influence from cloud and its shadow, the cloud and its shade are manually erased.

In Figure 4, the results of NDLI on the two dates are shown. For ease of interpretation of the NDLI results, the LULC classification shown in Figure 3 as to be considered. The blank part is the cloud and shadow, which is removed from the image. The built-up area and bare soil show an almost negative NDLI value. The vegetation area shows a relative higher value, from 0 to 0.15, the surface water has an even higher value.

According to the Equation 2, LST can be calculated based on the TIRS (Band 10) of Landsat 8 data collection-2 level-2. The spatial distribution of LST in Kelvin (K) on the two dates is shown in Figure 5. The cloud and its shade are manually erased as well.

From the results shown above, on 14th January 2019 and 30th January 2019, high LST values are found in the built-up region and bare soil region. The vegetation region and surface water show relatively low LST values.

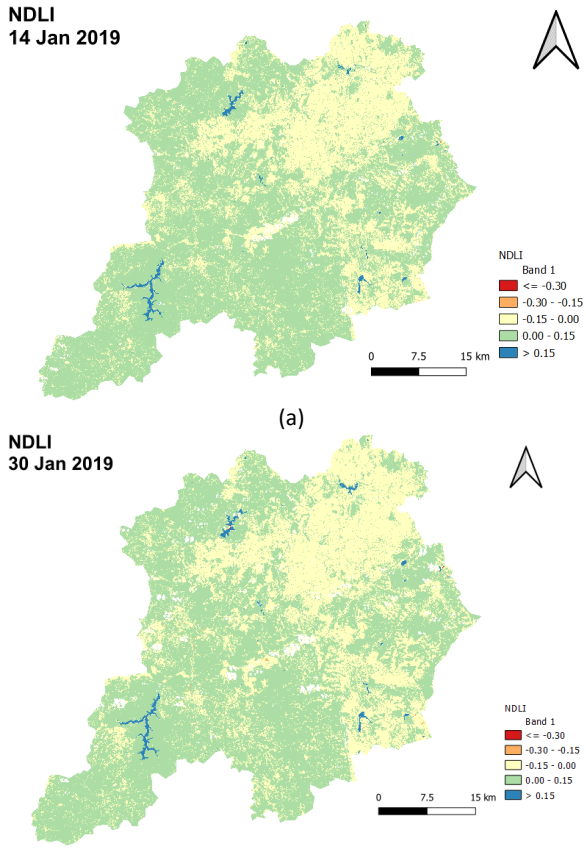


Figure 4. Results of NDLI: a) result on 14th Jan 2019; b) result on 30th Jan 2019.

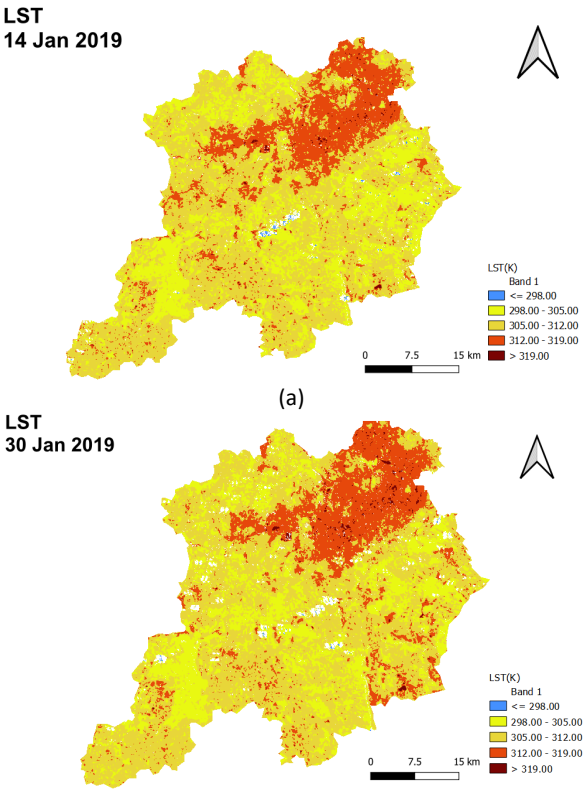


Figure 5. Results of LST: a) result on 14th Jan 2019; b) result on 30th Jan 2019.

C. *NDLI-LST triangle space*

Based on the result of the NDLI and LST, the NDLI-LST triangle space can be generated. According to the Equations 3-5, the results of NDLI-LST triangle space are shown in Figure 6.

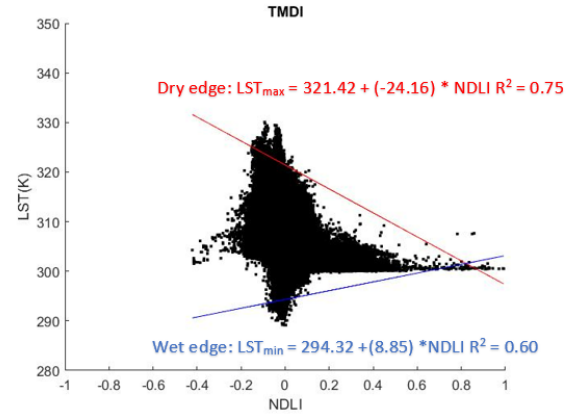


(a)

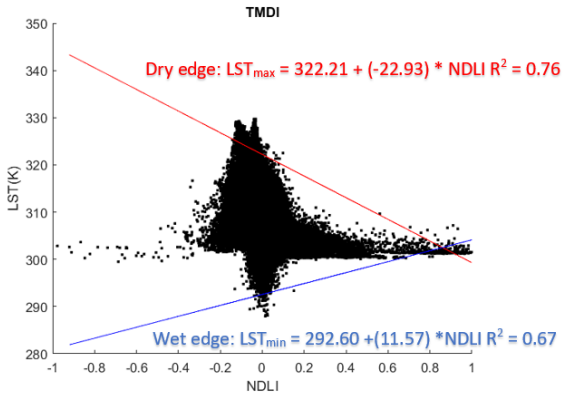


(b)

Figure 6. NDLI-LST triangle space: a) NDLI-LST space triangle on 14th Jan 2019; b) NDLI-LST triangle space on 30th Jan 2019.

In Figure 6, the red line is the dry edge while the blue line is the wet edge. On the dry edge, $LST_{max}$ shows a negative relation with NDLI. $R^2$ is 0.75 and 0.76 for the data from 14th January 2019 and 30th January 2019, respectively. For the wet edge, $LST_{min}$ shows a positive relation with NDLI. The $R^2$ is 0.60 and 0.67 on 14th January 2019 and 30th January 2019, respectively.

With the NDLI-LST triangle space, the results of TMDI can be calculated. According to the Equations 3-5, the results of TMDI are shown in Figure 7.

On 14th January 2019 and 30th January 2019, the built-up region shows high TMDI values. Because TMDI has negative correlation with soil moisture like TVDI, based on this, it was obvious that the built-up region had low soil moisture. The vegetation region shows relative high soil moisture, especially the vegetation close to surface water has high soil moisture.

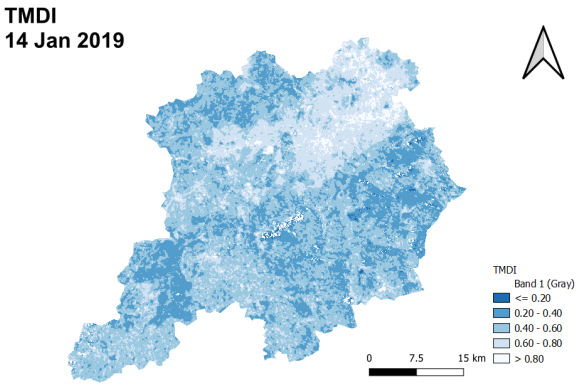


(a)

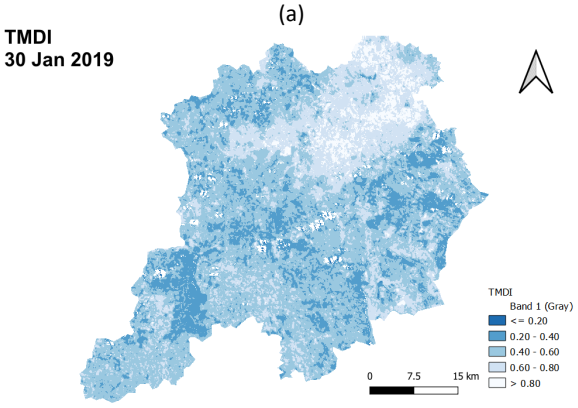


(b)

Figure 7. Results of TMDI with the classification schema introduced in Table 3: a) TMDI result from 14th Jan 2019; b) TMDI result from 30th Jan 2019.

D. *ET-based evaluation*

ET is derived from SEBAL. Which is used to assess the performance of the TMDI and the TVDI. The images of SEBAL-derived ET are shown in Figure 8.

The vegetation area and the surface water area show relatively high ET while the built-up area and bare soil show low ET.

Based on the LULC classification from Figure 3, the whole region is divided into 5 classes. Cloud and its shadow are excluded. The correlation coefficient between TMDI/TVDI and ET in different LULC classes is shown in the Table 4.

Table 4. Correlation coefficient between TMDI/TVDI and ET in different LULC classes

| | 14th Jan 2019 | | 30th Jan 2019 | |
|---|---|---|---|---|
| | TMDI | TVDI | TMDI | TVDI |
| ET (Whole area) | -0.65 | -0.57 | -0.70 | -0.51 |
| ET (Vegetation) | -0.47 | -0.43 | -0.54 | -0.47 |
| ET (Bare soil) | -0.48 | -0.49 | -0.51 | -0.58 |
| ET (Built-up) | -0.72 | -0.60 | -0.75 | -0.64 |

Overall speaking, TMDI performs better than TVDI based on the correlation coefficient with SEBAL-derived ET. For the whole region, the TMDI shows a negative correlation of -0.65 and -0.70 on those two dates. While the TVDI only shows a negative correlation of -0.57 and -0.51. For different types of LULC, in the built-up area, TMDI and TVDI have higher negative correlation with

SEBAL-derived ET, which have -0.72 and -0.60 on 14th January 2019 and -0.75 and -0.64 on 30th January 2019, respectively. In vegetation area those two indexes have a lower negative correlation with SEBAL-derived ET. In the vegetation region, the correlation coefficients between ET and TMDI are -0.47 and -0.54 on 14th on two dates. The correlation coefficients between ET and TVDI are: -0.43 and -0.47 on those two dates. The spatial distribution of the TMDI and the TVDI in the tailing dam is shown in Figure 9.

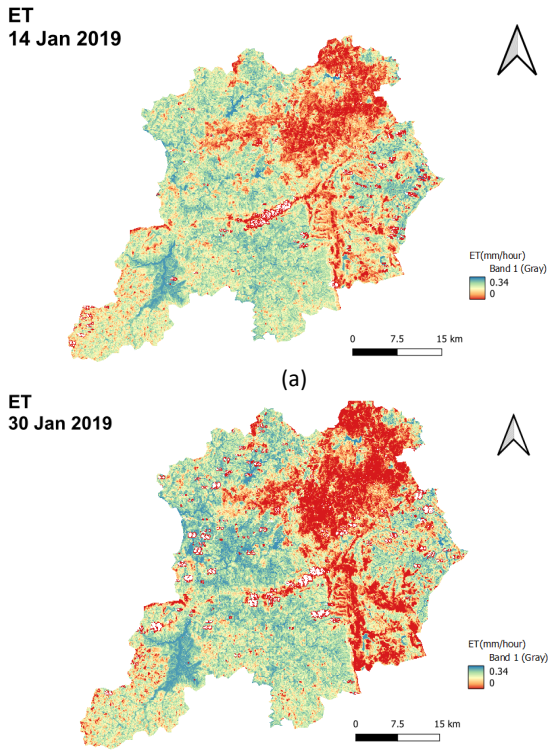


Figure 8. Results of ET combined with the LULC classification results from Figure 3: a) result on 14th Jan 2019; b) result on 30th Jan 2019.

The mean value of the TMDI and the TVDI in different tailing dam areas are shown in Table 5.

Table 5. Mean value of TVDI and TMDI in the tailing dam region

| | 14th Jan 2019 | | 30th Jan 2019 | |
|---|---|---|---|---|
| | TMDI | TVDI | TMDI | TVDI |
| i | 0.70 | 0.65 | 0.57 | 0.47 |
| ii | 0.56 | 0.55 | 0.45 | 0.39 |
| iii | 0.50 | 0.54 | 0.52 | 0.51 |
| iv | 0.31 | 0.37 | 0.34 | 0.41 |

Figure 9a and Figure 9c show the results for 14th January 2019, what is before the collapse of the tailing dam in Brumadinho. The border between (ii) tailings and (iv) region around tailings has a high soil moisture content, which is shown by the index ranging from 0.2 to 0.4. (iv) Region around tailings also shows high soil moisture (0.2 to 0.4). In Figure 9a, (iv) Region around tailings even has TMDI below 0.2. Those areas may have possibility to induce soil liquefaction.

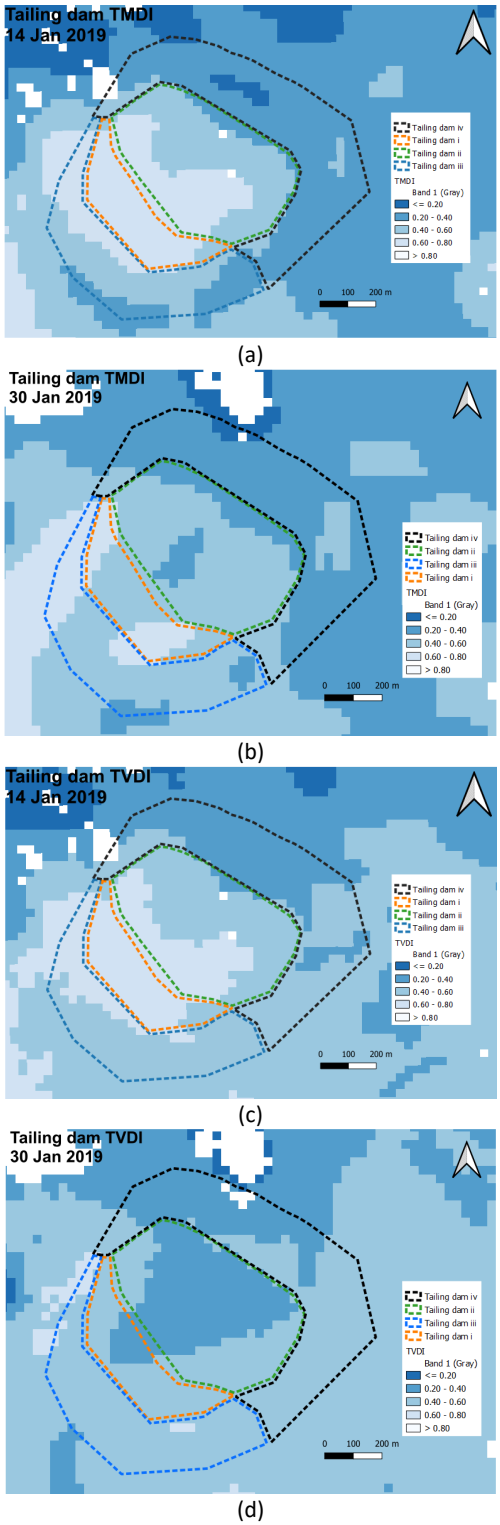


Figure 9. Spatial distribution of the TMDI and the TVDI in the tailing dam area: a) TMDI result on 14th Jan 2019; b) TMDI result on 30th Jan 2019; c) TVDI result on 14th Jan 2019; d) TVDI result on 30th Jan 2019.

Figure 9b and Figure 9d show the results for 30th January 2019, what is after the collapse of the tailing dam, the internal soil of the tailing dam is already exposed. The soil moisture in region (i) dam is increased according to TVDI and TMDI. The TMDI and the TVDI in

region (ii) tailings reached 0.2 to 0.4. Which can also indirectly verify the soil moisture in this region.

From Table 5 can be seen, that (iv) region around tailings has the highest soil moisture. On 14th January 2019 in (iv) region around tailings, the mean TMDI and TVDI are 0.31 and 0.37, respectively. On 30th January 2019, mean TMDI and TVDI are 0.34 and 0.41, respectively. After the collapse of the tailing dam, the mean soil moisture in (i) dam and (ii) tailings increases. In (iii) region around dam and (iv) region around tailings a different situation can be seen: in (iii) region around dam based on TVDI the soil moisture increases while based on TMDI the soil moisture decreases. In (iv) region around tailings both the TMDI and the TVDI show a decrease of the soil moisture.

## V. CONCLUSION

This study aims to use a new index, the TMDI to estimate the soil moisture of the tailing dam in Brumadinho, Brazil. Based on the Landsat 8 data on 14th January 2019 and 30th January 2019, one data is captured before the collapse of the tailing dam while another is captured after the collapse of the tailing dam, the soil moisture and the potential reason of the collapse of the tailing dam can be analyzed. Considering the whole region of Brumadinho and its surrounding areas for the calculation will increase the robustness of the TMDI.

In order to a better understanding, the distribution of land surface characteristics and LULC classification is used to classify the whole study region and divide the study area into five classes. With the sample to verify, the results show a good classification. The overall accuracy on the two dates are 95.67% and 94.11%. By using the OLI and TIRS from Landsat 8 data, NDLI and LST are calculated. The TMDI can be calculated based on the NDLI-LST triangle space. The TMDI is compared with the existing TVDI based on SEBAL-derived ET. The results show, that TMDI has much higher correlation with ET than TVDI, which means this index performs better. In different land type, in the built-up area, the correlation coefficient between ET and TMDI is higher than that in the bare soil and vegetation.

In the spatial distribution of the TMDI and TVDI, the tailing dam is divided into four parts. In the border between (ii) tailings and (iv) region around tailings a relative high soil moisture is presented. Besides, the (iv) region around tailings, which is fully covered with vegetation, also shows high soil moisture. It means that these areas have potential to induce soil liquefaction. In the thermal environment, the TMDI shows importance in the estimation of the soil moisture. It can be a very useful indicator to monitor soil moisture not only in mining field but also in the agriculture and forestry domain.

## References


Gama, F., Mura, J.C., R. Paradella, G. de Oliveira, (2020). Deformations Prior to the Brumadinho Dam Collapse Revealed by Sentinel-1 InSAR Data Using SBAS and PSI Techniques. In *Remote Sens*. Vol 12, No.21, pp. 3664.

Geofabrik. (2018). OpenStreetMap Data Extracts. Retrieved March 5th, 2022, from https://download.geofabrik.de/

Google. (n.d.). Google map. Retrieved March 4th, 2022, from http://www.google.cn/maps/vt?lyrs=s@820&gl=cn&x={x}&y={y}&z={z}

Laipelt, L., Kayser, R. H. B., Fleischmann, A. S., Ruhoff, A., Bastiaanssen, W., Erickson, T. A., and Melton, F. (2021). Long-term monitoring of evapotranspiration using the SEBAL algorithm and Google Earth Engine cloud computing. *ISPRS Journal of Photogrammetry and Remote Sensing*, 178, pp. 81-96.

Le, M. S., and Liou, Y. A. (2021a). Spatio-temporal assessment of surface moisture and evapotranspiration variability using remote sensing techniques. *Remote Sensing*, 13(9), 1667.

Le, M. S., and Liou, Y. A. (2021b). Temperature-Soil Moisture Dryness Index for Remote Sensing of Surface Soil Moisture Assessment. *IEEE Geoscience and Remote Sensing Letters*, 19, 1-5.

Liou, Y. A., Le, M. S., and Chien, H. (2018). Normalized difference latent heat index for remote sensing of land surface energy fluxes. *IEEE Transactions on Geoscience and Remote Sensing*, 57(3), pp. 1423-1433.

Qiu, G. Y., LI, H. Y., Zhang, Q. T., Wan, C. H. E. N., Liang, X. J., and Li, X. Z. (2013). Effects of evapotranspiration on mitigation of urban temperature by vegetation and urban agriculture. Journal of Integrative Agriculture, 12(8), pp. 1307-1315.

Rotta, L. H. S., Alcantara, E., Park, E., Negri, R. G., Lin, Y. N., Bernardo, N., and Souza Filho, C. R. (2020). The 2019 Brumadinho tailings dam collapse: Possible cause and impacts of the worst human and environmental disaster in Brazil. *International Journal of Applied Earth Observation and Geoinformation*, 90, 102119.

Sha, S., Ni, G., Yaohui, L., Tao, H. A. N., and Yanxia, Z. H. A. O. (2014). Introduction of application of temperature vegetation dryness index in China. Journal of Arid Meteorology, 32(1), 128.

USGS. (2022). EarthExplorer. Retrieved January 05th, 2022, from https://earthexplorer.usgs.gov/

USGS. (2022). Landsat Collection 2 Level-2 Science Products. Retrieved March 01st, 2022, from https://www.usgs.gov/landsat-missions/landsat-collection-2-level-2-science-products

Zare, M., Drastig, K., and Zude-Sasse, M. (2019). Tree water status in apple orchards measured by means of land surface temperature and vegetation index (LST–NDVI) trapezoidal space derived from Landsat 8 satellite images. *Sustainability*, Vol 12, No.1, pp.70.